AFRL-RZ-WP-TP-2012-0140

CURRENT SHARING BETWEEN SUPERCONDUCTING FILM AND NORMAL METAL (POSTPRINT)

George A. Levin, Paul N. Barnes, and John S. Bulmer

Mechanical Energy Conversion Branch
Energy/Power/Thermal Division

FEBRUARY 2012

AIR FORCE RESEARCH LABORATORY
PROPULSION DIRECTORATE
WRIGHT-PATTERSON AIR FORCE BASE, OH 45433-7251
AIR FORCE MATERIEL COMMAND
UNITED STATES AIR FORCE

REPORT DOCUMENTATION PAGE

Form Approved
OMB No. 0704-0188

1. REPORT DATE *(DD-MM-YY)*	2. REPORT TYPE	3. DATES COVERED *(From - To)*
February 2012	Journal Article Postprint	04 April 2005 – 04 April 2007

4. TITLE AND SUBTITLE
CURRENT SHARING BETWEEN SUPERCONDUCTING FILM AND NORMAL METAL (POSTPRINT)

5a. CONTRACT NUMBER
In-house

5b. GRANT NUMBER

5c. PROGRAM ELEMENT NUMBER
62203F

6. AUTHOR(S)
George A. Levin, Paul N. Barnes, and John S. Bulmer (AFRL/RZPG)

5d. PROJECT NUMBER
3145

5e. TASK NUMBER
32

5f. WORK UNIT NUMBER
314532ZE

7. PERFORMING ORGANIZATION NAME(S) AND ADDRESS(ES)
Mechanical Energy Conversion Branch (AFRL/RZPG)
Energy/Power/Thermal Division
Air Force Research Laboratory, Propulsion Directorate
Wright-Patterson Air Force Base, OH 45433-7251
Air Force Materiel Command, United States Air Force

8. PERFORMING ORGANIZATION REPORT NUMBER
AFRL-RZ-WP-TP-2012-0140

9. SPONSORING/MONITORING AGENCY NAME(S) AND ADDRESS(ES)
Air Force Research Laboratory
Propulsion Directorate
Wright-Patterson Air Force Base, OH 45433-7251
Air Force Materiel Command
United States Air Force

10. SPONSORING/MONITORING AGENCY ACRONYM(S)
AFRL/RZPG

11. SPONSORING/MONITORING AGENCY REPORT NUMBER(S)
AFRL-RZ-WP-TP-2012-0140

12. DISTRIBUTION/AVAILABILITY STATEMENT
Approved for public release; distribution unlimited.

13. SUPPLEMENTARY NOTES
Journal article published in *Superconductor Science and Technology*, Vol. 20, 2007.

 Work on this effort was completed in 2007. This paper has color content

PA Case Number: AFRL/WS 07-0797; Clearance Date: 04 Apr 2007.

14. ABSTRACT
A two-dimensional model is introduced that describes DC current sharing between the superconducting and normal metal layers in a configuration typical of YBCO-coated conductors. The model is used to compare the effectiveness of a surround stabilizer and a more conventional one-sided stabilizer. When the resistance of the interface between the superconductor and the stabilizer is low enough, the surround stabilizer is less effective than the one-sided stabilizer in stabilizing a hairline crack in the superconducting film.

15. SUBJECT TERMS
two-dimensional model, superconducting, metal layers, coated conductors, stabilizer, conventional, resistance, crack, film

16. SECURITY CLASSIFICATION OF:			17. LIMITATION OF ABSTRACT:	18. NUMBER OF PAGES	19a. NAME OF RESPONSIBLE PERSON (Monitor)
a. REPORT	b. ABSTRACT	c. THIS PAGE			Timothy J. Haugan
Unclassified	Unclassified	Unclassified	SAR	14	19b. TELEPHONE NUMBER *(Include Area Code)* N/A

Supercond. Sci. Technol. **20** (2007) 757–764 doi:10.1088/0953-2048/20/8/006

Current sharing between superconducting film and normal metal

George A Levin, Paul N Barnes and John S Bulmer

Propulsion Directorate, Air Force Research Laboratory, 1950 Fifth Street, Building 450, Wright-Patterson Air Force Base, OH 45433, USA

Received 7 March 2007, in final form 22 April 2007
Published 18 June 2007
Online at stacks.iop.org/SUST/20/757

Abstract
A two-dimensional model is introduced that describes DC current sharing between the superconducting and normal metal layers in a configuration typical of YBCO-coated conductors. The model is used to compare the effectiveness of a surround stabilizer and a more conventional one-sided stabilizer. When the resistance of the interface between the superconductor and the stabilizer is low enough, the surround stabilizer is less effective than the one-sided stabilizer in stabilizing a hairline crack in the superconducting film.

(Some figures in this article are in colour only in the electronic version)

1. Introduction

Coated conductors are one of the most promising candidates for the broader commercialization of high-T_c superconductors. The architecture of coated conductors can be described as a 'sandwich' in which the $YBa_2Cu_3O_{7-x}$ (YBCO) superconducting film of thickness about 1 μm is enclosed between a metal substrate of relatively high resistivity (Ni–5%W alloy, Hastelloy, or stainless steel) and a copper stabilizer layer [1–5]. The purpose of the stabilizer is to carry the transport current over the parts of the superconducting film that become temporarily or even permanently damaged or heated. An understanding of the processes and control of the characteristics of the current exchange between the superconductor and copper stabilizer is essential for developing effective stabilization of the conductor.

In coated conductors the superconducting film is deposited on a buffered metal substrate and the stabilizer is either soldered or electroplated on top of the YBCO film. Depending on the method by which the stabilizer is attached to the superconducting film, a thin layer of variable chemical composition is formed as a resistive interface between them. The interface resistance is thought to be determined by a few 'dead' (underdoped) unit cells of YBCO which has high normal state resistivity in the c-direction [6]. The spatial scale of the current exchange depends on the relationship between the interfacial resistance and the thickness and resistivity of the stabilizer. A one-dimensional model that describes such current exchange is well known. Here we have generalized it to a two-dimensional version. The model is then used to determine the effectiveness of a 'surround stabilizer'.

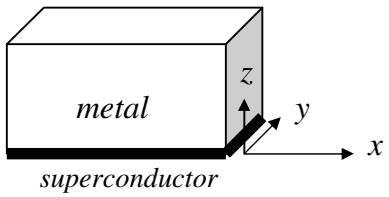

Figure 1. Diagram of a metal layer attached to a superconducting film.

Section 2 of this paper introduces a planar model of DC voltage distribution in the stabilizer, which is a two-dimensional generalization of the one-dimensional model that has been in use for some time [7–13]. In section 3 we compare the effectiveness of two different types of stabilizers—a 'one-sided stabilizer' [1] and a 'surround stabilizer' [2, 3]. Our conclusion is that for stabilization of hairline fractures in the superconducting layer the one-sided stabilizer is more effective than the surround stabilizer. This is true especially when the interface resistance is relatively low, so that the spatial scale of the current exchange is much smaller than the width of the conductor.

2. Planar model

Let us consider a layer of a normal metal in contact with a superconducting film (figure 1). Let $\bar{R}$ (with dimensionality Ω cm^2) be the resistivity of the interface between them, d the thickness of the metal and ρ the resistivity of the metal. Here

we consider only DC electric field and currents. The density of current inside the normal metal

$$\vec{j} = -\rho^{-1}\nabla\tilde{V}, \tag{1}$$

where $\tilde{V}(x, y, z)$ is the electric potential. By virtue of current conservation, $\mathrm{div}\,\vec{j} = 0$, the potential is determined by the three-dimensional (3D) Laplace equation:

$$\Delta\tilde{V} = 0. \tag{2}$$

At the superconductor–metal interface, the potential is subject to the boundary condition that follows from the ohmic relationship between the current and voltage across the interface:

$$j_z|_{z=0} = -\rho^{-1}\left.\frac{\partial\tilde{V}}{\partial z}\right|_{z=0} = -\frac{V - V_s}{\bar{R}}. \tag{3}$$

Here $V(x, y) \equiv \tilde{V}|_{z=0}$ is the value of the potential just above the interface and V_s is the potential of the superconducting film below the interface. The second boundary condition at $z = d$ depends on whether there are current leads attached to the stabilizer. If there are no current leads in the area of consideration, the boundary condition at $z = d$ is

$$\left.\frac{\partial\tilde{V}}{\partial z}\right|_{z=d} = 0. \tag{4}$$

The effect of the current leads attached to the stabilizer can be accounted for by changing the boundary condition (4) as follows:

$$-\rho^{-1}\left.\frac{\partial\tilde{V}}{\partial z}\right|_{z=d} = j(x, y). \tag{5}$$

Here $j(x, y)$ is a given density of current injected through the leads.

2.1. Stabilizer

A significant simplification of the model can be achieved in a practically important limit when the variation of the potential across the thickness of the stabilizer is small. Then, we can use Taylor's expansion to approximate $\tilde{V}(x, y, z)$ as follows:

$$\tilde{V}(x, y, z) \approx V(x, y) + \alpha z + \beta z^2. \tag{6}$$

The coefficients α and β are determined by the boundary conditions (3)–(5). With the boundary conditions (3) and (4) (no current leads attached) the potential takes the form:

$$\tilde{V}(x, y, z) = V + (V - V_s)\frac{z}{a} - (V - V_s)\frac{z^2}{2da}, \tag{7}$$

where a is a characteristic length scale:

$$a = \frac{\bar{R}}{\rho}. \tag{8}$$

The approximation (7) is valid as long as $d \ll a$. Another, less formal, way to interpret the criterion of validity of the planar approximation (7) is that the main resistance to current exchange is presented by the interface resistance, rather than by the vertical resistance of the stabilizer: $\rho d \ll \bar{R}$. Substituting the potential (7) in equation (2), and taking after the differentiation the limit $z \to 0$, we obtain for $V(x, y)$ the 2D Helmholtz equation:

$$\Delta V - \kappa^2(V - V_s) = 0. \tag{9}$$

Here $\kappa \equiv \lambda^{-1}$ defines a screening length

$$\lambda = (ad)^{1/2} = \left(\frac{d\bar{R}}{\rho}\right)^{1/2}. \tag{10}$$

The current can flow in the stabilizer only over distances of the order of λ. Everywhere else the stabilizer and superconducting film are equipotential and the current flows only in the superconducting layer.

The average value of the potential

$$V_{av}(x, y) = \frac{1}{d}\int_0^d \tilde{V}(x, y, z)\,dz \tag{11}$$

is given by

$$V_{av}(x, y) - V_s = (V - V_s)\left(1 + \frac{d}{3a}\right), \tag{12}$$

and as long as $d \ll a$, the variation of the potential across the thickness of the metal can be neglected when we estimate losses and other average quantities.

With current leads attached to the stabilizer we use the boundary condition (5) instead of the condition (4), and the potential takes form:

$$\tilde{V}(x, y, z) = V + (V - V_s)\frac{z}{a} - (V - V_s)\frac{z^2}{2da} - \rho j\frac{z^2}{2d}. \tag{13}$$

Then, equation (2) morphs into the 2D inhomogeneous Helmholtz equation for $V(x, y)$:

$$\Delta V - \kappa^2(V - V_s) = \frac{\rho}{d}j(x, y). \tag{14}$$

The applicability of the approximation (13) requires

$$\rho j \sim (V - V_s)/a. \tag{15}$$

Taking into account equations (3) and (8) this means that the density of current injected into the stabilizer from the leads should not substantially exceed the density of current exchanged between the stabilizer and the superconductor:

$$j \sim \frac{V - V_s}{\bar{R}}. \tag{16}$$

This in turn means that the size of the footprint of the current lead should not be much smaller than the screening length λ.

2.2. Superconductor

The equations describing the potential in the stabilizer have to be supplemented by the equations for the potential V_s in the superconducting film. It is reasonable to describe the superconducting film with thickness much smaller than

that of the stabilizer by a two-dimensional density of current $\vec{J}_s$ (A cm^{-1}) subject to the current conservation condition:

$$\nabla \cdot \vec{J}_s = -\, j_z|_{z=0} = \frac{V - V_s}{\bar{R}}. \tag{17}$$

Here we have used equation (3). A constituent relation for the superconductor can be written as $\vec{E} \equiv r(J_s)\vec{J}_s$, which translates into a nonlinear equation for the potential:

$$\nabla[r^{-1}(|\nabla V_s|)\nabla V_s] = -\frac{V - V_s}{\bar{R}}. \tag{18}$$

Using a power law dependence [14]

$$r(J_s) = \frac{E_0}{J_c}\frac{|J_s|^{n-1}}{|J_c|^{n-1}}, \tag{19}$$

equation (18) takes the form:

$$\nabla\left[\nabla V_s \left(\frac{|\nabla V_s|}{E_0}\right)^{(1-n)/n}\right] = \Lambda^{-2}(V - V_s). \tag{20}$$

Here J_c is the critical current density and $E_0 = 1\ \mu$V cm^{-1}. The screening length in the superconductor

$$\Lambda = \left(\frac{\bar{R}J_c}{E_0}\right)^{1/2}, \tag{21}$$

along with that in the stabilizer (equation (10)), determines the distances over which the current exchange between the superconductor and stabilizer takes place.

Measurements carried out on currently manufactured coated conductors [15] indicate that their interface resistivity is $\bar{R} \sim 50$ nΩ cm^2. At 77 K the resistivity of copper is $\rho \approx 0.2 \times 10^{-6}\ \Omega$ cm. The thickness of the stabilizer is $d \sim 20$–$40\ \mu$m. Thus, the characteristic length a defined by equation (8) is

$$a \sim 2.5 \text{ mm}, \tag{22}$$

and the condition of applicability of the planar model $d \ll a$ is well satisfied. The screening length in the stabilizer is

$$\lambda = (da)^{1/2} \sim 300\ \mu\text{m}. \tag{23}$$

With the critical current density in coated conductors $J_c \sim 200$–400 A cm^{-1}, the corresponding screening length in the superconductor is

$$\Lambda \sim 3\text{–}4 \text{ cm}. \tag{24}$$

A huge difference in these screening lengths can be understood as the difference between the sheet resistance of copper $\rho/d \sim 10^{-4}\ \Omega$ and the equivalent quantity $E_0/J_c \sim 10^{-8}\ \Omega$ in the superconducting film. Thus, the effects of the current exchange in the stabilizer manifest itself over much shorter distances than those in the superconductor. The potential difference between superconductor and stabilizer tends to be eliminated over distances of the order of λ because the stabilizer adjusts its potential to that of the superconductor.

The length scales of the potential distribution in the superconducting films tend to be large, of the order of bn or $bn^{1/2}$, in the transverse and longitudinal direction, respectively, where b is the size of a defect or an obstacle to current and $n \sim 20$–40 is the exponent in equation (19) [14]. Therefore, the details of the current exchange that takes place on the spatial scale of the order of λ in many situations can be accurately described by assuming that the potential of the superconductor is constant or piecewise constant. Generally, as a good approximation, one can neglect the right-hand side in equation (20) and determine the potential V_s as if there were no current exchange with the stabilizer [14]. Then, the solution of equation (9) is given by

$$V(x, y) = -\kappa^2 \int G(x - x', y - y')V_s(x', y')\,dx'\,dy', \tag{25}$$

where $G(x - x', y - y')$ is the Green's function of the Helmholtz equation. The accuracy of this approximation is of the order of λ/Λ and can be improved by iteration.

2.3. Energy losses

There are several general statements about energy losses that follow from the planar model. The power dissipation has three components. First is the dissipation in the stabilizer:

$$Q_{st} = \int \rho^{-1}|\nabla\tilde{V}|^2\,dx\,dy\,dz \approx \frac{d}{\rho}\int |\nabla V|^2\,dx\,dy. \tag{26}$$

Second is the power dissipation in the interface itself (equation (3)):

$$Q_{int} = -\int j_z|_{z=0}\,(V - V_s)\,dx\,dy = \int \frac{(V - V_s)^2}{\bar{R}}\,dx\,dy. \tag{27}$$

The third is the power loss in the superconductor:

$$Q_s = -\int \vec{J}_s \cdot \nabla V_s\,dx\,dy. \tag{28}$$

One can easily show that equation (9) can be obtained by a variational method as a condition of minimization of the power loss $Q_1 = Q_{st} + Q_{int}$:

$$\frac{\delta Q_1}{\delta V} = 0, \tag{29}$$

provided that the variation $\delta V(x, y) = 0$ at the boundaries and the potential V_s is not varied.

If we multiply equation (9) by $(V - V_s)d/\rho$, we get

$$d/\rho \int (V - V_s)\Delta V\,dx\,dy = Q_{int}. \tag{30}$$

The integrand in the left-hand side can be rewritten as follows:

$$(V - V_s)\Delta V = \nabla \cdot ((V - V_s)\nabla V) - \nabla V \cdot \nabla(V - V_s). \tag{31}$$

At the boundaries of the conductor either $\nabla V = 0$ or $V - V_s \to 0$. Therefore, taking into account equation (26), we obtain

$$Q_{st} + Q_{int} = d/\rho \int \nabla V \cdot \nabla V_s\,dx\,dy \equiv \int (\vec{J}_n \cdot \vec{E}_s)\,dx\,dy. \tag{32}$$

Here $\vec{J}_n$ and $\vec{E}_s$ are the $2D$ density of current in the stabilizer and the electric field in the superconductor, respectively.

Similarly, multiplying equation (17) by $V - V_s$ and taking into account equation (28) we get

$$Q_s + Q_{int} = -\int \nabla V \cdot \vec{J}_s\,dx\,dy \equiv \int (\vec{J}_s \cdot \vec{E}_n)\,dx\,dy. \tag{33}$$

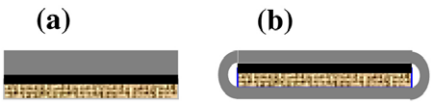

Figure 2. (a) Diagram of the cross-section of a YBCO-coated conductor with 'one-sided' stabilizer. The superconducting film (thick black line) is deposited on a buffered substrate and covered with copper stabilizer. (b) 'Surround stabilizer'—a copper layer encapsulates the substrate and YBCO film. Only the top (the front) part of the stabilizer is directly attached to the superconducting film.

The right-hand sides of equations (32) and (33) look deceptively similar to the conventional Joule heat expressions, except that the current density and electric field are from different layers. These relations may be more useful in evaluating losses in coated conductors on the basis of numerical models or magneto-optical imaging than equations (26)–(28). In the areas where the superconductor and metal are equipotential, the electric field $\vec{E}_s = \vec{E}_n$ and equations (32), (33) become the conventional Joule heat expressions because there is no current across the interface and no loss in the interface.

3. Coated conductor stabilizer

As a first application of the planar model we will consider the stabilizing properties of two types of stabilizers for coated conductors. The simplest, shown in figure 2(a), is a layer of copper of the same width as that of the YBCO film soldered or electroplated on top of the silver covered superconducting film (let us call it a *one-sided stabilizer*) [16]. However, two of the main companies leading the development of coated superconductors (American Superconductor and SuperPower) have opted for a different type of stabilizer—the *surround* stabilizer, shown in figure 2(b) [2, 3]. Among the advantages of this architecture is that copper encapsulates and protects the YBCO film and the substrate. If the edges of the surround stabilizer are rounded, it reduces the stray electric field, which is important for high voltage applications.

Implicit in these arguments in favour of the surround stabilizer is an assumption that in terms of its ability to exchange current with the superconducting layer it is equivalent to the one-sided stabilizer with the same total thickness. This assumption needs to be critically examined. In this section we will compare the effectiveness of these two types of stabilizers using the planar model described above.

3.1. One-sided stabilizer

A thin superconducting film consisting of a multitude of carefully aligned grains is especially vulnerable to the proliferation of microcracks that limit the local critical current. Even when a newly manufactured conductor is devoid of such current limiting obstacles, they may appear as the result of stresses applied to the conductor during the coil winding and its subsequent exploitation in rotating machinery or magnets. Even a relatively short crack creates a magnetic flux jet—a region of enhanced electric field that spans over a distance about n times greater than the length of the crack (n is the exponent in equation (19)) [14]. Therefore, the hairline cracks may turn out to be one of the main types of defect that will determine the limits of reliability of the coated conductors over their lifetime.

Let us consider a specific situation when DC current flows through the coated conductor and the superconducting layer is disrupted by a hairline fracture, be it a permanent physical fracture or a linear hot spot. Then, the transport current will be diverted into the stabilizer over the fracture and return back to the superconductor. As was discussed above, a good approximation of this situation can be a piecewise constant potential V_s of the superconducting film. An implicit condition for that is that the critical current remains greater than the transport current even at the elevated temperature caused by excessive dissipation. Let the long axis of the tape be the x-axis, and the fracture be located at $x = 0$, figure 1. Let us choose the potential of the superconducting layer $V_s = \delta V/2$ for $x > 0$ and $V_s = -\delta V/2$ for $x < 0$. Here δV is the potential difference between the distant points of the conductor that is required to maintain the current across the fracture in the superconducting film. Correspondingly, the solution of equation (9) has the form:

$$V = \pm\frac{\delta V}{2}(1 - e^{-\kappa|x|}). \tag{34}$$

The signs $\pm$ refer, respectively, to $x > 0$ and $x < 0$. The electric field is given by

$$E_x = -\frac{\partial V}{\partial x} = -\frac{\kappa\delta V}{2}e^{-\kappa|x|}. \tag{35}$$

This is the value of the electric field at $z = 0$. The electric field averaged over the thickness of the stabilizer differs by a factor $(1 + d/3a)$ (see equation (12)).

The total current in the stabilizer is given by

$$I = \frac{d}{\rho}\int |E_x|\,dy\Big|_{x=0} = \frac{\delta V W d}{2\lambda\rho} \equiv \frac{\delta V}{R}, \tag{36}$$

where W is the width of the conductor and

$$R = \frac{2\rho\lambda}{Wd} \tag{37}$$

is the effective resistance of the hairline fracture. The power dissipated in the stabilizer is

$$Q_{st} = \frac{Wd}{\rho}\int |E_x|^2\,dx = \frac{1}{2}\frac{\delta V^2}{R}. \tag{38}$$

Small corrections of the order of d/a, are neglected here. Power is also dissipated in the interface itself:

$$Q_{int} = -\int j_z(V - V_s)\,dx\,dy = \int \frac{(V - V_s)^2}{\bar{R}}\,dx\,dy = \frac{1}{2}\frac{\delta V^2}{R}. \tag{39}$$

Here we have used equations (26) and (27). As expected, the total power loss is simply

$$Q_1 = Q_{st} + Q_{int} = \delta V I = RI^2 = \frac{\delta V^2}{R}. \tag{40}$$

It is instructive to realize that half of the total energy dissipation takes place in the very thin (in comparison

with the thickness of the stabilizer) interface between the superconductor and copper. In fact, in the one-dimensional case not only is the total dissipation equally divided between the stabilizer and interface, but the areal density of the power dissipation is as well:

$$\frac{d}{\rho}\left(\frac{\mathrm{d}V}{\mathrm{d}x}\right)^2 = \frac{(V - V_s)^2}{\bar{R}}.$$

In other words, the thermal load that the conductor experiences is not uniformly distributed in the stabilizer. Given that the YBCO film is only about 1 μm thick, the energy dissipated in its interface may increase temporarily the temperature of the superconducting film substantially above that of the stabilizer. This raises a possibility that the YBCO film may be damaged during the quench event even when the temperature of the stabilizer remains within the safety limit (below room temperature).

The result given by equation (40) can be directly obtained from equation (32). The electric field in the superconductor with the piecewise constant potential is $|E_s| = \delta V \delta(x)$, so that from equation (32) it follows that $Q_1 = \delta V I$. For a 4 mm wide coated conductor the resistance of a hairline fracture or a hot spot given by equation (37) is:

$$R \sim 7.5\ \mu\Omega. \tag{41}$$

For the transport current $I \sim 100$ A the power dissipation is

$$Q = RI^2 \sim 75\ \mathrm{mW}. \tag{42}$$

3.2. *Partial fracture*

For completeness, let us also consider a situation when a hairline crack in the superconducting film does not completely inhibit the flow of the transport current through the superconducting film. In other words, let us assume that the fracture is a hairline region with a finite critical current $I_c < I$. Outside of this hairline anomaly the critical current $I_c' > I$. This model may be considered as an approximation of a faceted grain boundary with alternating segments of different critical current density J_c [14].

Then, over the anomaly, the excess of current $I - I_c$ will be diverted into the stabilizer. Equations (34) and (35) are still valid, but equation (36) takes form

$$I - I_c = \frac{d}{\rho}\int |E_x|\,\mathrm{d}y\Big|_{x=0} = \frac{\delta V W d}{2\lambda\rho} \equiv \frac{\delta V}{R}.$$

Power loss in the stabilizer and interface are given by equations (38) and (39):

$$Q_{st} = Q_{int} = \frac{1}{2}\frac{\delta V^2}{R} = \frac{1}{2}R(I - I_c)^2.$$

The power dissipated in the superconducting film is

$$Q_s = \int (\vec{J}_s \cdot \vec{E}_s)\,\mathrm{d}x\,\mathrm{d}y = I_c \delta V = RI_c(I - I_c).$$

Here we have used $|E_s| = \delta V \delta(x)$. The total power dissipation is

$$Q_{tot} = Q_{st} + Q_{int} + Q_s = \delta V I = RI(I - I_c).$$

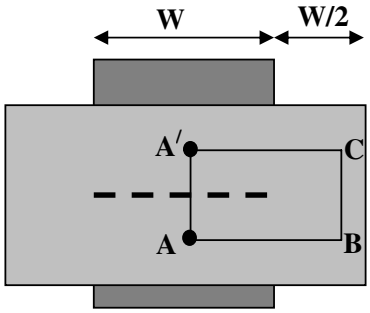

Figure 3. Diagram of a tape-like conductor of width W. The back side of the stabilizer shown in figure 2(b) is cut along the centreline and unfolded forming two flaps of width $W/2$ each. The dashed line indicates a fracture in the superconducting film that forces transport current into the stabilizer.

Since the thickness of the superconducting film is small in comparison to that of the stabilizer, the heat dissipated in the interface may strongly affect the temperature of the superconducting film before spreading out throughout the stabilizer. In contrast, the power dissipated in the stabilizer itself is distributed uniformly over the stabilizer volume. The amount of power dissipation that directly affects the temperature of the superconducting film is

$$Q_2 = Q_s + Q_{int} = \tfrac{1}{2}R(I^2 - I_c^2).$$

The ratio of the power dissipation in the stabilizer to that in the superconducting film is

$$\frac{Q_{st}}{Q_2} = \frac{(I - I_c)^2}{I^2 - I_c^2}.$$

Thus, in the case of the partial fracture the total dissipated energy is reduced in comparison with the complete fracture in proportion to $I - I_c$, but a greater part of this dissipation is strongly localized in the superconducting film. For example, if $I_c = (2/3)I$, only 20% of the total dissipation is released in the stabilizer. The remaining 80% of the heat is deposited in the superconducting film and the interface with potentially significant consequences for the dynamics of stabilization and quench development.

3.3. *Surround stabilizer*

In the surround stabilizer (figure 2(b)) only the front part of it is in electric contact with the superconducting film. The back side of the stabilizer can exchange current with the front side and with the superconductor only through the edges because the substrate is insulated from the YBCO by the buffer layer. This point is better illustrated in figure 3. Imagine that the back side of the stabilizer is cut along the centreline and unfolded, forming flaps. The effectiveness of the surround stabilizer depends on how fully the current fills the back side (the flaps in figure 3) in the situation when the superconducting layer is disrupted, as was described in the previous subsection. One can easily see a potential problem with the effectiveness of the flaps. Consider two points A and A′ separated by a distance 2λ and with a potential difference between them of δV. Then consider another contour A–B–C–A′ that extends deep into the

back side of the stabilizer. The potential difference $\delta V = -\oint \vec{E} \cdot \mathrm{d}\vec{\ell}$ is the same along any contour. In the currently manufactured conductors the length of the ABCA′ contour is approximately $W + 2\lambda \gg 2\lambda$ (equation (23)). Therefore, the electric field in the back side (and the density of current) must be substantially smaller than that in the front side by a factor of approximately λ/W.

Analytically, the problem of the surround stabilizer can be formulated as follows. The front side and the back side can be treated as two tape-like sheets of copper of equal thickness located within the range $-\infty < x < \infty$, $-W/2 < y < W/2$. The potential in the front side $V(x, y)$ is described by equation (9). The potential in the back side $U(x, y)$ has to satisfy the 2D Laplace equation:

$$\Delta U = 0. \tag{43}$$

The two solutions have to be matched at the boundaries $y = \pm W/2$:

$$\left.\frac{\partial V}{\partial x}\right|_{y=\pm W/2} = \left.\frac{\partial U}{\partial x}\right|_{y=\pm W/2}, \tag{44}$$

and

$$\left.\frac{\partial V}{\partial y}\right|_{y=\pm W/2} = -\left.\frac{\partial U}{\partial y}\right|_{y=\pm W/2}, \tag{45}$$

In addition, $x = 0$ (the location of the fracture) must be an equipotential line with the same potential for both sides:

$$V(x, y)|_{x=0} = U(x, y)|_{x=0} = \text{const}. \tag{46}$$

A complete solution of equations (9) and (43)–(46) can be obtained by a straightforward, albeit cumbersome, procedure and will be presented elsewhere. However, for practical conductors this problem is characterized by a small parameter $\lambda/W \ll 1$ ($\kappa W \gg 1$). Taking advantage of this, we can find the solution perturbatively. As an initial approximation $V^{(0)}$ we take the solution of equation (9) in the form (34) and (35). The solution for the back side of the stabilizer we seek in the form

$$U^{(1)}(x, y) = \int_{-\infty}^{\infty} U_k^{(1)} \cosh(ky) \mathrm{e}^{\mathrm{i}kx} \frac{\mathrm{d}k}{(2\pi)^{1/2}}. \tag{47}$$

The Fourier transform $U_k^{(1)}$ is determined by the boundary condition (44):

$$\int_{-\infty}^{\infty} \mathrm{i}k U_k^{(1)} \cosh(kW/2) \mathrm{e}^{\mathrm{i}kx} \frac{\mathrm{d}k}{(2\pi)^{1/2}} = \frac{\kappa \delta V}{2} \mathrm{e}^{-\kappa|x|}. \tag{48}$$

From this follows:

$$\mathrm{i}k U_k^{(1)} \cosh(kW/2) = \frac{\delta V}{(2\pi)^{1/2}} \frac{\kappa^2}{k^2 + \kappa^2}. \tag{49}$$

The x-component of the electric field $E_x^{(1)} = -\partial U^{(1)}/\partial x$ is given by:

$$E_x^{(1)} = -\frac{\delta V}{(2\pi)^{1/2}} \int_{-\infty}^{\infty} \frac{\cosh(ky)}{\cosh(kW/2)} \frac{\kappa^2}{k^2 + \kappa^2} \mathrm{e}^{\mathrm{i}kx} \frac{\mathrm{d}k}{(2\pi)^{1/2}}. \tag{50}$$

Correspondingly, the y-component of the electric field is

$$E_y^{(1)} = -\mathrm{i}\frac{\delta V}{(2\pi)^{1/2}} \int_{-\infty}^{\infty} \frac{\sinh(ky)}{\cosh(kW/2)} \frac{\kappa^2}{k^2 + \kappa^2} \mathrm{e}^{\mathrm{i}kx} \frac{\mathrm{d}k}{(2\pi)^{1/2}}. \tag{51}$$

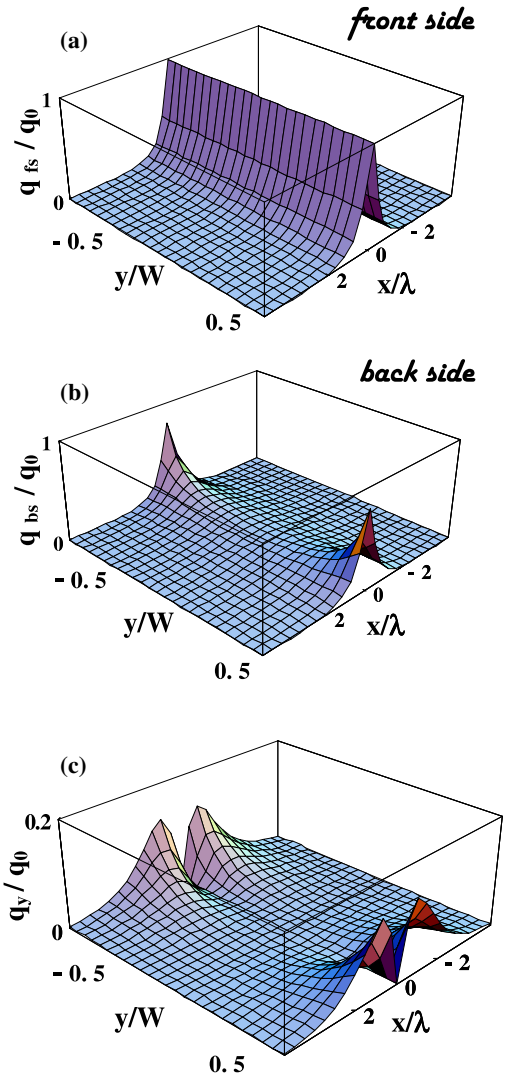

Figure 4. (a) The areal density of power dissipation in the front side of the stabilizer (equation (53)). (b) The areal density of power dissipation in the back side (equation (55)). (c) The distribution of the transverse current (equation (56)). The power dissipation is normalized by the value q_0 (equation (54)). The x-coordinate (along the transport current) is normalized by the screening length λ; the transverse coordinate is normalized by the width of the conductor W.

We can now compare the power loss in the front side of the stabilizer to that in the back side. The areal density of power dissipation in the front side is

$$q_{\mathrm{fs}} = 2\frac{d}{\rho} E_x^2. \tag{52}$$

The factor 2 accounts for the dissipation in the stabilizer itself (equation (38)) and in the interface (equation (39)). Using equation (35) we obtain:

$$q_{\mathrm{fs}} = \frac{d}{\rho} \frac{\delta V^2}{2\lambda^2} \mathrm{e}^{-2\kappa|x|}. \tag{53}$$

Figure 4(a) shows the areal density of the power loss given by equation (53), normalized by its maximum value

$$q_0 = \frac{d}{\rho} \frac{\delta V^2}{2\lambda^2}. \tag{54}$$

In the back side of the stabilizer the areal density of dissipation is given by

$$q_{\rm bs} = \frac{d}{\rho}(E_x^2 + E_y^2), \tag{55}$$

where E_x and E_y are given by equations (50) and (51). The total amount of power dissipated in the back side and its spatial distribution (figure 4(b)) is determined by the value of κW. The distribution shown in figure 4(b) corresponds to $\kappa W = 5$. For $W = 4$ mm, this is equivalent to $\lambda = 800$ μm. For the value of $\lambda \approx 300$ μm measured in [15], $\kappa W \approx 13$, so that the amount of power dissipated in the back side is smaller than that shown in figure 4(b). For comparison, in figure 4(c) the density of dissipation attributable to the y-component of the current density flowing into and out of the back side from the front side through the edges is also shown:

$$q_y = \frac{d}{\rho}E_y^2. \tag{56}$$

The discontinuity in the areal density of power dissipation at the edges, $y = \pm W/2$, between the front side and the back side (figures 4(a), (b)), is not the result of approximation. The density of power dissipated in the metal itself is continuous, by virtue of the boundary conditions (44) and (45), but additional power is dissipated in the interface in the front side. Therefore, the total dissipation in the front side is greater than that in the back side as long as there is current exchange across the interface. The difference between the amount of power dissipated in the two sides increases with increasing κW.

In order to evaluate the total resistance of the hairline fracture and compare it with that for the one-sided stabilizer (equation (37)), let us consider the total current that passes through the back side of the stabilizer:

$$I_{\rm bs} = \frac{d}{\rho}\int_{-W/2}^{W/2} E_x \,{\rm d}y, \tag{57}$$

where E_x is taken at $x = 0$. Carrying out integration with E_x given by equation (50) we obtain:

$$I_{\rm bs} = \frac{2\delta V d}{\rho(2\pi)^{1/2}}\int_{-\infty}^{\infty}\tanh(kW/2)\frac{\kappa^2}{k^2+\kappa^2}\frac{1}{k}\frac{{\rm d}k}{(2\pi)^{1/2}}. \tag{58}$$

Introducing a dimensionless variable $\xi = k/\kappa$, we get:

$$I_{\rm bs} = \frac{2\delta V d}{\pi\rho}\int_0^{\infty}\tanh(\xi\kappa W/2)\frac{1}{\xi^2+1}\frac{{\rm d}\xi}{\xi}. \tag{59}$$

Taking into account that

$$\int\frac{{\rm d}\xi}{\xi(1+\xi^2)} = \ln\frac{\xi}{(1+\xi^2)^{1/2}}, \tag{60}$$

and integrating equation (59) by parts, we obtain:

$$I_{\rm bs} = -\frac{2\delta V d}{\pi\rho}\frac{\kappa W}{2}\int_0^{\infty}\frac{{\rm d}\xi}{\cosh^2(\xi\kappa W/2)}\ln\frac{\xi}{(1+\xi^2)^{1/2}}. \tag{61}$$

In the limit $\kappa W \gg 1$

$$\begin{aligned} I_{\rm bs} &\approx -\frac{2\delta V d}{\pi\rho}\frac{\kappa W}{2}\int_0^{\infty}\frac{{\rm d}\xi\ln\xi}{\cosh^2(\xi\kappa W/2)} \\ &= \frac{2\delta V d}{\pi\rho}(\ln(\kappa W/2) - \Psi(1/2) - \ln\pi) \\ &= \frac{2\delta V d}{\pi\rho}\ln(1.13\kappa W). \end{aligned} \tag{62}$$

Here $\Psi(1/2) \approx -1.96$ [17]. The total current in the stabilizer is the sum of the current flowing in the front side (equation (36)), and the back side (equation (62)), is

$$I = \frac{\delta V W d}{2\lambda\rho}\left(1 + \frac{4}{\pi}\frac{\ln(1.13\kappa W)}{\kappa W}\right). \tag{63}$$

Thus, when the screening length $\lambda \ll W$, which is characteristic of the state of the art coated conductors, the back side of the stabilizer carries a relatively small fraction of the total current. For example, if we take the value of $\lambda = 300$ μm (equation (23)) and $W = 4$ mm ($\kappa W \approx 13$), the current in the back side is equal to a quarter of that in the front side.

Correspondingly, the resistance of the hairline fracture stabilized by the surround stabilizer is

$$R_{\rm ss} = \frac{\delta V}{I} \approx \frac{2\rho\lambda}{Wd}\left(1 - \frac{4}{\pi}\frac{\ln(1.13\kappa W)}{\kappa W}\right). \tag{64}$$

The effectiveness of the surround stabilizer is important. In the currently manufactured coated conductors the back side takes up as much space as the front side, and therefore decreases the engineering current density as much as the front side, but only partially contributes to stabilization of the hairline fractures. Using previous estimates for a surround stabilizer consisting of 20 μm copper sheet (the total thickness of copper is 40 μm), we have to conclude that for this specific type of defect its stabilizing property (the resistance $R_{\rm ss}$) is the same as that of a 25 μm one-sided stabilizer (equation (37)).

This conclusion does not apply to the situation when the length of the normal zone is greater than or of the order of the width of the conductor. Then the current flowing in the stabilizer fills both sides of the stabilizer more or less uniformly. However, this corresponds to quench when stability has already been breached. It should be emphasized that in most experiments in which the stability of coated conductors has been tested so far, the dominant scenario is the creation of the initial normal zone of a fairly large area [18]. In these situations there is little difference between the stabilizing properties of the one-sided and surround stabilizers. The effectiveness of the stabilizer with respect to the initial hairline fracture has not yet been addressed experimentally.

4. Summary and suggestion

The planar model that describes the DC current sharing between the superconducting film and adjacent metal, including the expressions for energy dissipation (33) and (34), may become a useful addition to the powerful analytical [14] and numerical methods that have been developed to study the current distribution in superconducting films, allowing them to be expanded to practical coated conductors.

One noteworthy conclusion of our analysis is that when the DC current is forced from the superconductor into the stabilizer as much as half of the total energy dissipation takes place in the very thin interface on the surface of the superconducting film (equation (39)). As a result, the temperature of the superconducting film may increase temporarily above the room temperature and cause irreversible damage to the film. The temperature at the top of the stabilizer, where it is usually measured during an experiment, may remain within the safety limits at all times.

The surround stabilizer is not as effective as the one-sided stabilizer in the case of a hairline fracture if the screening length is small in comparison to the width of the conductor. Therefore, in order to stabilize coated conductors against all potential perturbations, including hairline cracks, the total thickness of copper in a surround stabilizer would have to be greater than that in a one-sided stabilizer. Since high engineering current density is a major potential competitive advantage of coated conductors over conventional copper wires, this shortcoming needs to be corrected. An obvious solution is to use an asymmetric surround stabilizer, where the front side has a greater thickness than the back side. This retains the advantages of the surround stabilizer configuration such as encapsulation of the YBCO film by copper and the possibility of rounding the edges. At the same time the total thickness of copper can be reduced because the main contribution to stabilization is provided by the front part of the stabilizer. An additional bonus of the asymmetric architecture of the surround stabilizer is that it places the YBCO film closer to the neutral axis.

Acknowledgments

We thank T Haugan and C Varanasi for useful discussions.

References

[1] Larbalestier D, Gurevich A, Feldman D M and Polyanskii A 2001 *Nature* **414** 368
[2] Schoop U *et al* 2005 *IEEE Trans. Appl. Supercond.* **15** 2611–6
[3] Xie Y-Y *et al* 2005 *Physica* C **426–431** 849–57
[4] Iijima Y, Kakimoto K, Sutoh Y, Ajimura S and Saitoh T 2005 *IEEE Trans. Appl. Supercond.* **15** 2590
[5] Usoskin A, Rutt A, Knoke J, Krauth H and Arndt Th 2005 *IEEE Trans. Appl. Supercond.* **15** 2604
[6] Angurel L A, Bona M, Andres J M, Munoz-Rojas D and Casan-Pastor N 2005 *Supercond. Sci. Technol.* **18** 135
[7] Fang Y, Danyluk S, Cha Y S and Lanagan M T 1996 *J. Appl. Phys.* **79** 947
[8] Polak M, Parrell W J, Cai X Y, Polyanskii A, Hellstrom E E, Larbalestier D C and Majoros M 1997 *Supercond. Sci. Technol.* **10** 769–77 and references therein
[9] Cesnak L, Kovac P and Gomory F 2000 *Supercond. Sci. Technol.* **13** 1450
[10] Usoskin A, Issaev A, Freyhardt H C, Leghissa M, Oomen M P and Neumueller H-W 2002 *Physica* C **372–376** 857–62
[11] Fu Y, Tsukamoto O and Furuse M 2003 *IEEE Trans. Appl. Supercond.* **13** 1780
[12] Stenvall A, Korpela A, Lehtonen J and Mikkonen R 2007 *Supercond. Sci. Technol.* **20** 92 and references therein
[13] Takàcs S 2007 *Supercond. Sci. Technol.* **20** 180
[14] Friesen M and Gurevich A 2001 *Phys. Rev.* B **63** 064521
[15] Polak M, Barnes P N and Levin G A 2006 *Supercond. Sci. Technol.* **19** 817
[16] Kim K, Paranthaman M, Norton D P, Aytug T, Cantoni C, Gapud A A, Goyal A and Christen D K 2006 *Supercond. Sci. Technol.* **19** R23
[17] Gradshteyn I S and Ryzhik I M 1980 *Table of Integrals, Series and Products* (San Diego, CA: Academic)
[18] Wang X, Trociewitz U P and Schwartz J 2007 *J. Appl. Phys.* **101** 053904 and references therein